How to cite: *Angew. Chem. Int. Ed.* **2022,** *61,* e202117006
International Edition: doi.org/10.1002/anie.202117006
German Edition: doi.org/10.1002/ange.202117006

Rhodium Catalysis

Rhodium-NHC-Catalyzed *gem*-Specific *O*-Selective Hydropyridonation of Terminal Alkynes

María Galiana-Cameo, Raúl Romeo, Asier Urriolabeitia, Vincenzo Passarelli, Jesús J. Pérez-Torrente, Victor Polo, and Ricardo Castarlenas**

Abstract: The dinuclear complex $[Rh(\mu\text{-}Cl)(\eta^2\text{-coe})(IPr)]_2$ is an efficient catalyst for the *O*-selective Markovnikov-type addition of 2-pyridones to terminal alkynes. DFT calculations support a hydride-free pathway entailing intramolecular oxidative protonation of a π-alkyne by a κ^1N-hydroxypyridine ligand. Subsequent *O*-nucleophilic attack on a metallacyclopropene species affords an *O*-alkenyl-2-oxypyridine chelate rhodium intermediate as the catalyst resting state. The release of the alkenyl ether is calculated as the rate-determining step.

The 2-pyridone scaffold can be found in many biologically relevant compounds, including some drugs approved by the FDA for the treatment of cancer, HIV or pulmonary fibrosis (Scheme 1).[1] Classical multistep synthetic procedures[2] have been gradually substituted by more efficient metal-catalyzed approaches.[3] Thus, while reactivity on the *C*-sites mainly rely on C–H activation,[4] a diverse set of methods for heteroatomic functionalization have been described, including alkylation with organohalides,[5] the use of diazo compounds,[6] addition to unsaturated substrates,[7] or allylic substitution reactions.[8] However, the *N*- vs. *O*-selectivity is far to be controlled and critically depends on the reaction conditions or the ligands, partly as a result of 2-hydroxypyridine vs. 2-pyridone tautomerization.[9]

In particular, preparation of *O*- or *N*-alkenylated 2-pyridones presents unique challenges, especially for the *gem*-olefin derivatives (Scheme 2). Firstly, the access via the *O*-nucleophilic attack of enolates to 2-halogenated-pyridines is hampered. In addition, thermodynamically preferred *N*-substituted *trans*-isomers are prevalent when using alkenyl halides or boronic acids.[10] Other synthetic approaches, such as isomerization within an *O*-unsaturated chain,[11] *O*- to *N*-rearrangement,[12] or aldol condensation,[13] have limited generality lacking the formation of *gem*-isomers. The few existing preparative methods for *gem*-alkenyl pyridones involve multistep procedures[14] or the use of specific precursors such as tosylhydrazones[15] or benzynes,[16] therefore more reliable synthetic methods are desirable. In this context, the Markovnikov-addition of 2-pyridones to triple bonds seems a straightforward atom-economical access.

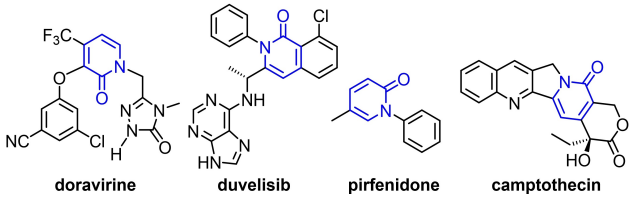

Scheme 1. Some 2-pyridone-based drugs approved by the FDA.

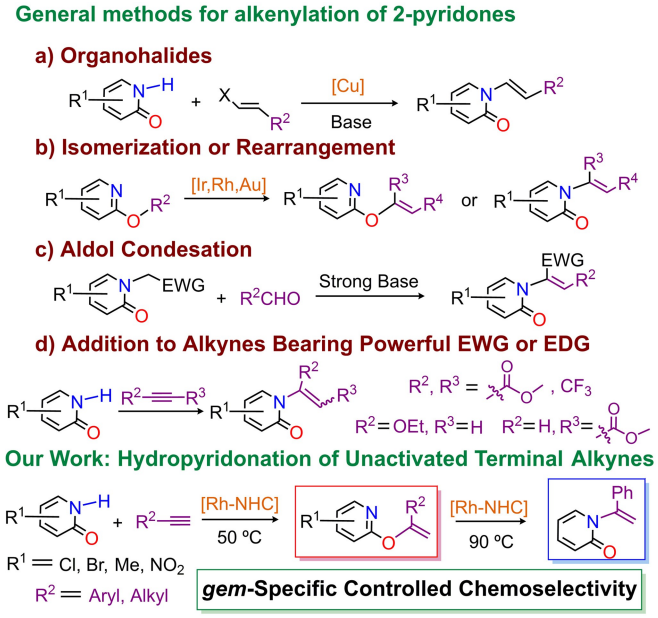

Scheme 2. Previous reports for preparation of *N*- or *O*-alkenylated 2-pyridones and our strategy.

[*] M. Galiana-Cameo, R. Romeo, Dr. V. Passarelli, Prof. Dr. J. J. Pérez-Torrente, Dr. R. Castarlenas
Departamento de Química Inorgánica-Instituto de Síntesis Química y Catálisis Homogénea (ISQCH),
Universidad de Zaragoza-CSIC,
C/Pedro Cerbuna 12, CP, 50009 Zaragoza (Spain)
E-mail: rcastar@unizar.es

A. Urriolabeitia, Prof. Dr. V. Polo
Departamento de Química Física, Universidad de Zaragoza,
C/Pedro Cerbuna 12, CP, 50009 Zaragoza (Spain)
E-mail: vipolo@unizar.es

However, direct addition proceeds only for alkynes bearing powerful EWG or EDG groups,[17] thus, we envisage a transition-metal catalyzed approach for unactivated terminal alkynes. Moreover, we anticipate the different affinity of rhodium for *O*- or *N*-donor functions as a potential tool to control chemoselectivity. Nevertheless, an important handicap for successful catalytic alkyne *hydropyridonation* is the intrinsic high self-reactivity of terminal alkynes to give a myriad of dimeric, polymeric or cyclic structures.[18]

Our research group has recently disclosed efficient rhodium-*N*-heterocyclic carbene (NHC) catalysts for diverse carbon-heteroatom couplings via hydrofunctionalization of alkynes.[19] Particularly, the introduction of 2-pyridone in the Rh-NHC framework results in impressive TOFs for alkyne dimerization.[20] The 2-pyridonato ligand behaves as a fast proton shuttle between the two alkynes. Moreover, the specific *gem*-selectivity of 1,3-enynes arises from the preferred protonation at the terminal position of a π-coordinated alkyne. In the course of mechanistic studies involving $[Rh(\mu\text{-}Cl)(\eta^2\text{-coe})(IPr)]_2$ (**1**) {IPr = 1,3-bis-(2,6-diisopropylphenyl)imidazolin-2-carbene; coe = cyclooctene}, 2-pyridone, and phenylacetylene, we serendipitously observed the formation of a new Rh-IPr complex in small quantities. This compound has now been identified by X-ray diffraction analysis and multinuclear NMR spectroscopy as RhCl(IPr)-$[\kappa N,\eta^2\text{-}\{py\text{-}O\text{–}C(Ph)=CH_2\}]$ (**2**), featuring an unexpected *O*-alkenyl-2-oxypyridine chelate (Figure 1). Complex **2** was isolated in 79 % yield by treatment of **1** with stoichiometric amounts of phenylacetylene and 2-pyridone. In the solid state, coordination of the alkenyl ether is shown by Rh–N41 {2.0891(15) Å} and Rh–ct1 distances {1.96913(15) Å} (ct1, olefin centroid). Moreover, the appearance of two doublets of doublets, $\delta = 2.61$ ($J_{H\text{-}H} = 4.3$, $J_{H\text{-}Rh} = 2.8$ Hz) and 2.54 ppm ($J_{H\text{-}Rh} = 2.1$ Hz), in the ^{1}H NMR spectrum and two doublets, 103.8 ($J_{C\text{-}Rh} = 18.6$ Hz) and 31.5 ppm ($J_{C\text{-}Rh} = 15.5$ Hz), in the $^{13}C\{^1H\}$-APT NMR experiment, confirms the coordination of the geminal olefin in solution.

In view of the ability of **1** to promote the stoichiometric alkyne-pyridone C–O coupling, we next studied its application to catalytic alkyne hydropyridonation. Gratifyingly, the addition of **1**, 5 mol % of Rh, to the benchmark substrates 2-pyridone (**3a**) and phenylacetylene (**4a**) in $CDCl_3$ resulted in the formation of the *gem*-alkenyl ether 2-(1-phenylvinyl)oxypyridine (**5aa**), after 20 h at 40 °C, as the exclusive heterocoupling product. Only 8 % of the 1,3-enyne arisen from competitive alkyne dimerization was observed. Other polar solvents were tested but alkyne dimerization prevailed (see Supporting Information). Temperature screening revealed a gradual reduction of alkyne conversion over 50 °C, likely due to catalyst decomposition, thus further experiments were performed at this compromise temperature. Interestingly, complex **2** was detected in the first monitoring spectrum. Indeed, similar catalytic outcome was obtained by using **2** as catalyst. Both facts suggest that **2** might be the resting state of the catalytic cycle. Moreover, the presence of an NHC was disclosed to be essential. The precursor of **1**, $[Rh(\mu\text{-}Cl)(\eta^2\text{-coe})_2]_2$, was inactive, while the Wilkinson's catalyst $RhCl(PPh_3)_3$ or the in situ formed $[Rh(\mu\text{-}Cl)(BINAP)]_2$ favored alkyne dimerization vs. hydropyridonation. It is worth a mention of the work of Breit's group showing the Rh-BINAP compound as efficient catalyst for the 2-pyridone addition to allenes.[7a] Other Rh-IPr complexes with κ^2acetato or CO ancillary ligands were inefficient.

As for the scope of alkyne hydropyridonation promoted by **1**, catalytic reactions were monitored in NMR tubes using a 5 mol % of Rh and 1:1 pyridone:alkyne ratio in $CDCl_3$ at 50 °C (Figure 2). Organic products were isolated after 20 h (Scheme 3). In general, *gem*-specific *O*-alkenylated derivatives **5** were obtained, with the exception of 6-halogenated-2-pyridone substrates (**3e**,**f**), which also gave *N*-alkenylated products **6** in variable amounts. Competitive alkyne dimerization was limited to 1–12 % in cases of effective hydropyridonation, except for 4-(trifluoromethyl)phenylacetylene (**4d**) (20 %), which agrees with the faster alkyne dimerization previously observed for this alkyne.[20] Otherwise, inefficient substrates such as 6-methyl-2-pyridone or 2-quinolone produced higher amounts of 1,3-enyne. Regarding the functional groups, aromatic alkynes reacted faster than aliphatic ones, while no definite trend was observed for substituted 2-pyridones. The more divergent results were found for 6-substituted ones. Thus, 6-chloro-2-pyridone (**3f**) is the most

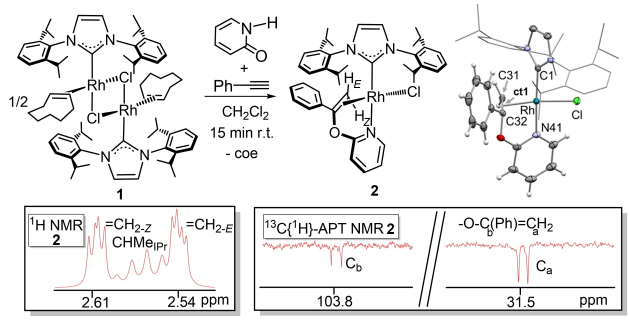

Figure 1. Formation of the chelate *O*-alkenyl-2-oxypyridine rhodium complex **2** and ORTEP view. For clarity a wireframe style is adopted for the NHC wingtips and most hydrogen atoms are omitted. Selected bond lengths [Å] are: Rh–C1 2.0193(18), Rh–Cl 2.3353(5), Rh–ct1 1.96913(15), C31–C32 1.408(3), Rh–N41 2.0891(15); ct1: centroid of C31 and C32.

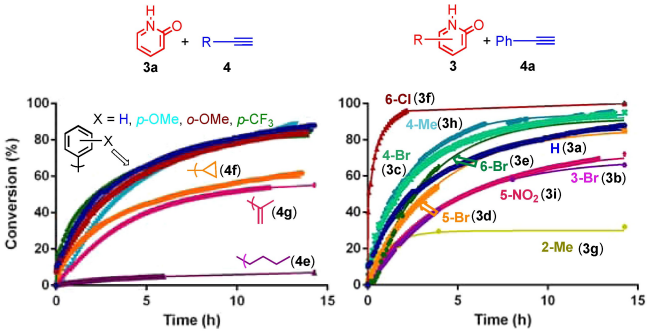

Figure 2. Reaction profile for the hydropyridonation of alkynes with 2-pyridone (left) and phenylacetylene with functionalized 2-pyridone derivatives (right).

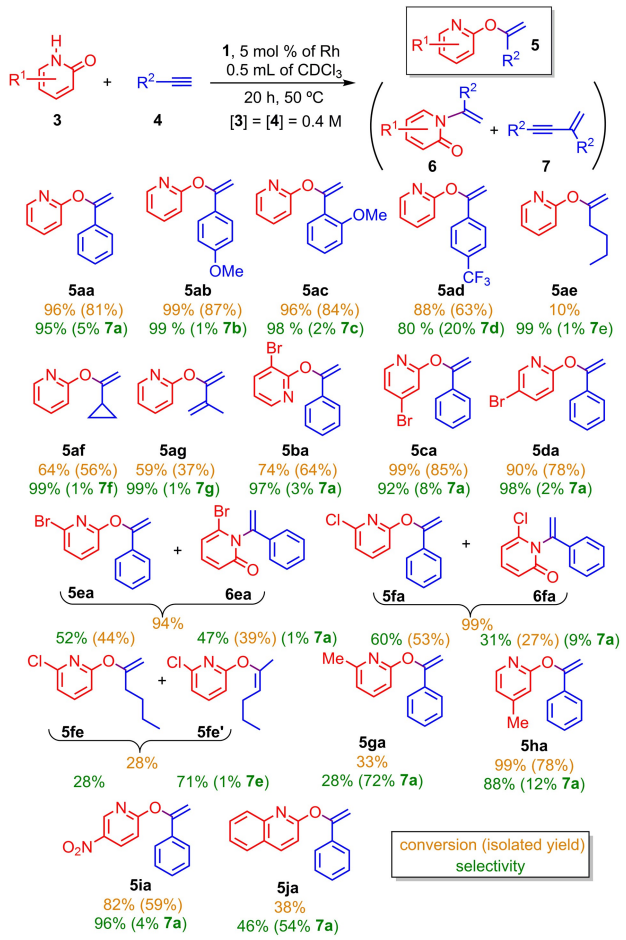

Scheme 3. Scope for the hydropyridonation of alkynes catalysed by **1**.

active substrate in this study, whereas poor conversion was obtained for 6-methyl-2-pyridone (**3g**), with the bromo counterpart **3e** lying in the middle. Substitution in other positions had only moderate influence. The alkenyl ether arising from 6-chloro-2-pyridone and 1-hexyne was obtained as a mixture of two isomers as a result of terminal to internal olefin isomerization. Finally, 4-methyl-2-pyridone (**3h**) slightly overcame the catalytic activity of parent 2-pyridone, while 5-nitro-2-pyridone (**3i**) fell behind. Other bulky, heteroatomic-substituted propargyl derivatives or internal alkynes were catalytically inefficient.

Some control experiments were performed to identify the reaction mechanism. Addition of 2-pyridone and phenylacetylene to **1** at −60 °C resulted in the immediate formation of complex **2** and no other intermediates, including Rh–H species, could be detected. Besides, H/D exchange between the *N*-deuterated 2-pyridone and the terminal proton of phenylacetylene preclude us from obtaining accurate information from deuterium labelling experiments (See Supporting Information). Catalytic tests in which 2-pyridone was replaced by phenol, *N*-methyl-2-aminopyridine, 2-thiopyridine, or 2-(hydroxymethyl)pyridine were unproductive, indicating that the presence of both N and O atoms located at 1,3-positions is essential.

The mechanism of the alkyne hydropyridonation catalyzed by **1** was studied by DFT computational analysis using 2-pyridone and phenylacetylene as model substrates (Figure 3, ΔG in kcal mol^{-1}). A plausible first step is the π-alkyne and κ^1*N*-hydroxypyridine coordination to the labile precursor **1** to yield **A**, which has been selected as the energetic reference. The O–H oxidative addition seems unfeasible since the corresponding Rh–H species **K**, located 13.7 kcal mol^{-1} above **A**, requires to surmount a barrier of 31.2 kcal mol^{-1} (see Figure S124 in Supporting Information). Alternatively, we propose a hydride-free pathway entailing oxidative protonation and reductive coupling steps (Scheme 4).[20,21] Thus, the κ^1*N*-hydroxypyridine ligand of **A** can behave as an intramolecular Brønsted acid able to protonate the terminal position of the π-alkyne to form the Rh^{III}-alkenyl species **B**, via **TSAB**. Protonation of internal position of the triple bond is disfavored

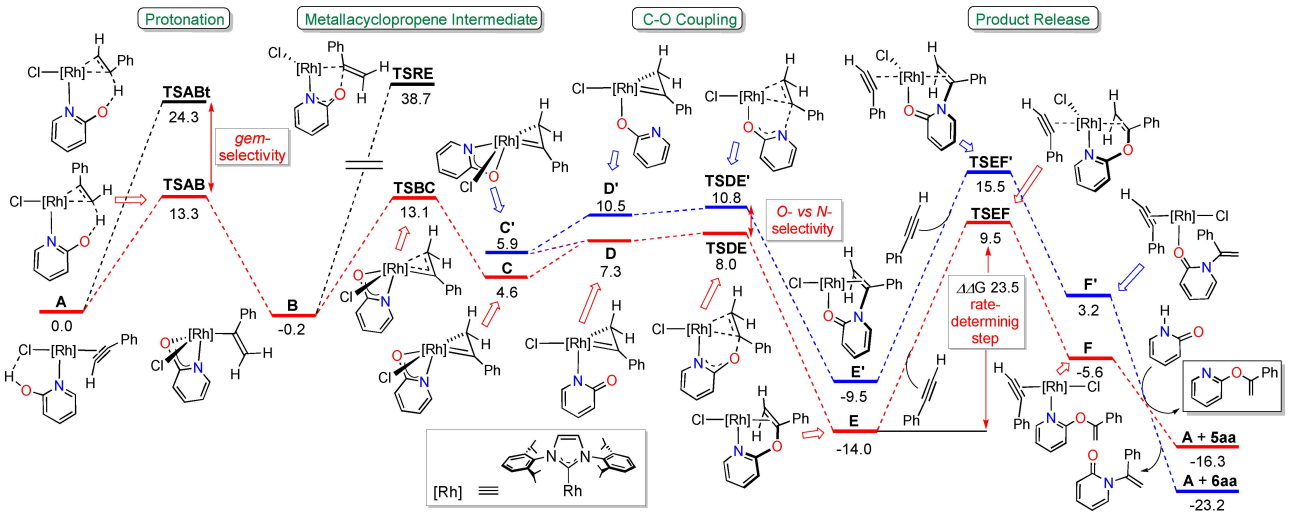

Figure 3. DFT energetic profile (ΔG in kcal mol^{-1}, relative to **A** and isolated molecules) along hydropyridonation of phenylacetylene. *O*-alkenylation, red pathway, and *N*-alkenylation, blue pathway.

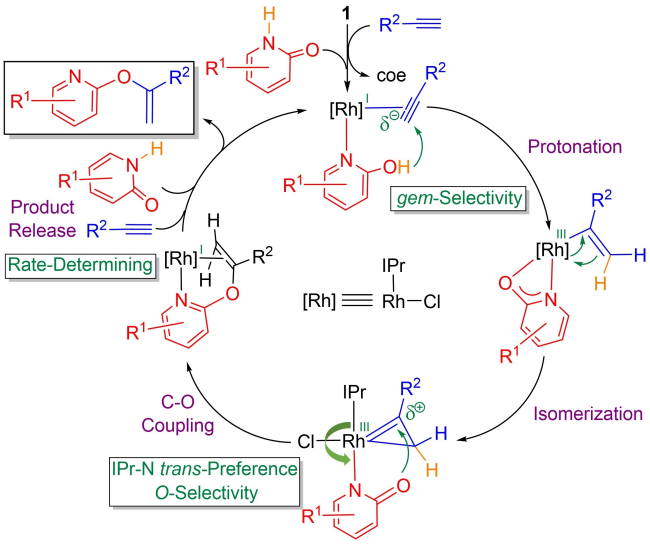

Scheme 4. Mechanistic proposal for alkyne hydropyridonation.

(**TSABt**, $\Delta\Delta G$ of 11.0 kcal mol^{-1}), which ultimately determines the high *gem*-selectivity.

The direct C–O reductive coupling within **B** was found to be unaffordable under catalytic conditions,[22] which is in sharp contrast to that observed for alkenyl-alkynyl C–C coupling in alkyne dimerization.[20] However, the isomerization of the alkenyl derivative **B** to the metallacyclopropene species **C**, though destabilized by 4.8 kcal mol^{-1}, opens an accessible pathway to the *O*-alkenyl-oxypyridine species **E** (−14.0 kcal mol^{-1}), in agreement with the isolation of **2**. This stage entails the decoordination of the oxygen atom of the pyridonato (**C**→**D**) and subsequent *O*-nucleophilic attack, in turn facilitated by increased positive charge at the carbenic carbon atom of the metallacyclopropene in **D** (see Figure S131 in Supporting Information).[21c,23] In contrast, the attack of the nitrogen atom has a higher barrier (**TSDE′**, $\Delta\Delta G$ 2.8 kcal mol^{-1}), in accordance with the preferential *O*-alkenylation. Most likely, the ultimate reason for the chemoselectivity could be the preferred coordination of a pyridine scaffold *trans* to IPr, thus causing a seesaw effect responsible of the *O*-nucleophilic attack.[24] Moreover, the particular stereoelectronic properties of the bulky powerful electron releasing IPr might play a role in the stabilization of metallacyclopropene species (See Figure S125 in Supporting Information for comparison with a PPh_3 analogue). In fact, these uncommon structures can be considered as essential intermediates in the *gem*-selective alkyne hydroalkoxylation in analogy to the role played by vinylidenes in the formation of *E*/*Z* isomers.[25]

The catalytic cycle ends with the associative release of the alkenyl ether (**TSEF**, 23.5 kcal mol^{-1}), which is the rate-determining step (see Figure S126 in Supporting Information). At this point, the interplay between steric hindrance and the high *trans* effect imparted by the NHC might trigger the release of the catalytic product from **2**.[19a] It is interesting to note that the final *N*-alkenyl product is more stable than the *O*-alkenyl one indicating a kinetic control under catalytic conditions. Calculations involving the 1-hexyne show a higher barrier of 25.9 kcal mol^{-1}, consistent with the slower reaction rate. Besides, the higher rate observed for 6-chloro-2-pyridone **3f** is likely due to steric effects, which might be responsible for the decrease of the product release barrier, whereas the similar energies of **5fa** and **6fa** account for the formation of both isomers (See Supporting Information).

Analysis of the energetic profiles of Figure 3 reveals that isomerization of *O*-alkenyl-oxypyridines to thermodynamically preferred *N*-alkenyl derivatives is feasible by breaking back the C–O bond (overall barrier for **A**+**5aa**→**C** via **TSEF**: 25.8 kcal mol^{-1}).[23a] Thus, heating isolated **5aa** or **5ia** in the presence of catalytic amounts of **1** for 72 h at 90 °C resulted in the formation of the *N*-alkenyl-pyridone derivatives **6** (Figure 4). Formation of **6** was not observed when simply heating the NMR tube containing crude **5** from catalytic hydropyridonation, likely due to decomposition of active species. In fact, the isomerization did not proceed either in the absence of **1** or using $[Rh(\mu\text{-}Cl)(\eta^2\text{-coe})_2]_2$ as catalyst. Given the small difference in the chemical shift of intuitively representative C_2-imidic (**5aa**, δ = 163.3 ppm) or C_2-amidic (**6aa**, δ = 162.2 ppm) atoms in the $^{13}C\{^1H\}$-APT NMR spectra, the 2D ^1H-^{15}N long-range HMQC NMR experiment was key to the characterization of **6**. Thus, correlation between one olefinic proton and the nitrogen atom was observed for **6**, but it is absent in **5** where both atoms are located five bonds away. Similarly to the formation of **2**, the *N*-alkenyl-pyridone derivative **6aa** reacts with **1** to yield RhCl[κ*O*,η^2-{C_4H_4(C=O)N}-C(Ph)=CH_2](IPr) (**8**). Multinuclear NMR data agree with the proposed pyridone-alkenyl structure exhibiting a κ^1*O*,η^2-coordination mode.

In conclusion, we have disclosed herein a Rh-NHC efficient catalytic system for *gem*-specific and *O*-selective alkyne hydropyridonation. Mechanistic studies in combination with DFT calculations support a hydride-free pathway. After initial coordination of both substrates, intramolecular oxidative protonation at the terminal position of a π-alkyne by a κ^1*N*-hydroxypyridine ligand is responsible for *gem*-specificity. Since direct C–O reductive elimination within the resulting alkenyl-pyridonato intermediate was found to be unaffordable, isomerization to a metallacyclopropene species opens the way to nucleophilic attack. Chemoselectivity control towards the less

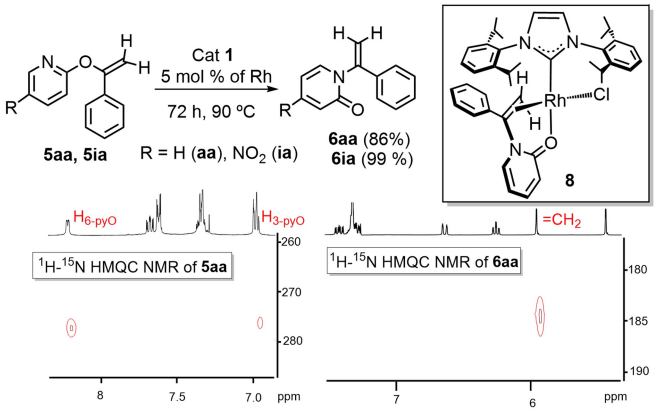

Figure 4. *O*- to *N*-alkenyl isomerization and ^1H-^{15}N HMQC NMR correlations.

thermodynamically favoured *O*-alkenylated products arises from the preferred *N*- vs. *O*-coordination of the κ^1pyridonato ligand in Rh-IPr systems. In addition, the key role of the bulky electron-releasing IPr ligand in the stabilization of the metallacyclopropene species has been identified. Research efforts are underway for the design of more efficient catalysts that will open future opportunities for functionalization of other biologically active heterocycles.

Acknowledgements

Financial support from the Spanish Ministerio de Ciencia e Innovación MCIN/AEI/10.13039/501100011033, under the Projects PID2019-103965GB-I00 and PGC2018-099383-B-I00, and the Departamento de Ciencia, Universidad y Sociedad del Conocimiento del Gobierno de Aragón (group E42_20R) is gratefully acknowledged.

Conflict of Interest

The authors declare no conflict of interest.

Data Availability Statement

The data that support the findings of this study are available from the corresponding author upon reasonable request.

Keywords: Alkenylation · Alkyne Hydrofunctionalization · C–O Coupling · N-Heterocyclic Carbene · Pyridone

[1] a) H. J. Jessen, K. Gademann, *Nat. Rev. Cancer* **2010**, *27*, 1168–1185; b) Y. Zhang, A. Pike, *Bioorg. Med. Chem. Lett.* **2021**, *38*, 127849.
[2] a) M. Torres, S. Gil, M. Parra, *Curr. Org. Chem.* **2005**, *9*, 1757–1779; b) J. G. Sośnicki, T. J. Idzik, *Synthesis* **2019**, *51*, 3369–3396.
[3] See for example: a) H. Imase, K. Noguchi, M. Hirano, K. Tanaka, *Org. Lett.* **2008**, *10*, 3563–3566; b) T. K. Hyster, T. Rovis, *Chem. Sci.* **2011**, *2*, 1606–1610; c) J.-F. Tan, C. T. Bormann, K. Severin, N. Cramer, *ACS Catal.* **2020**, *10*, 3790–3796.
[4] a) K. Hirano, M. Miura, *Chem. Sci.* **2018**, *9*, 22–32; b) A. Biswas, S. Mayti, S. Pan, R. Samanta, *Chem. Asian J.* **2020**, *15*, 2092–2109.
[5] a) R. A. Altman, S. L. Buchwald, *Org. Lett.* **2007**, *9*, 643–646; b) M. Kuriyama, N. Hanazawa, Y. Abe, K. Katagiri, S. Ono, K. Yamamoto, O. Onomura, *Chem. Sci.* **2020**, *11*, 8295–8300.
[6] a) G. Xu, P. Chen, P. Liu, S. Tang, X. Zhang, J. Sun, *Angew. Chem. Int. Ed.* **2019**, *58*, 1980–1984; *Angew. Chem.* **2019**, *131*, 2002–2006; b) J. Yang, G. Wang, H. Zhou, Z. Li, B. Ma, M. Song, R. Sun, C. Huo, *Org. Biomol. Chem.* **2021**, *19*, 394–398.
[7] a) C. Li, M. Kähny, B. Breit, *Angew. Chem. Int. Ed.* **2014**, *53*, 13780–13784; *Angew. Chem.* **2014**, *126*, 14000–14004; b) Y.-C. Wu, Y. Jhong, H.-J. Lin, S. P. Swain, H.-H. G. Tsai, D.-R. Hou, *Adv. Synth. Catal.* **2019**, *361*, 4966–4982.
[8] a) X. Zhang, Z.-P. Yang, L. Huang, S.-L. You, *Angew. Chem. Int. Ed.* **2015**, *54*, 1873–1876; *Angew. Chem.* **2015**, *127*, 1893–1896; b) S. Khan, B. H. Shah, I. Khan, M. Li, Y. J. Zhang, *Chem. Commun.* **2019**, *55*, 13168–13171.
[9] M. Breugst, H. Mayr, *J. Am. Chem. Soc.* **2010**, *132*, 15380–15389.
[10] a) P. S. Mariano, E. Krochmal, R. Beamer, P. L. Huesmann, D. Dunaway-Mariano, *Tetrahedron* **1978**, *34*, 2609–2616; b) Y. Bolshan, R. A. Batey, *Angew. Chem. Int. Ed.* **2008**, *47*, 2109–2112; *Angew. Chem.* **2008**, *120*, 2139–2142.
[11] a) X. Chew, Y. Lin, Y. H. Lim, *RSC Adv.* **2014**, *4*, 16765–16768; b) C. Sun, X. Qi, X.-L. Min, X.-D. Bai, P. Liu, Y. He, *Chem. Sci.* **2020**, *11*, 10119–10126.
[12] a) S. Z. Tasker, B. M. Brandsen, K. A. Ryu, G. S. Snapper, R. J. Staples, R. L. DeKock, C. E. Anderson, *Org. Lett.* **2011**, *13*, 6224–6227; b) G. Xu, Y. Shao, S. Tang, Q. Chen, J. Sun, *Org. Lett.* **2020**, *22*, 9303–9307.
[13] G. N. Shivers, F. C. Pigge, *J. Org. Chem.* **2021**, *86*, 13134–13142.
[14] J. Yang, G. B. Dudley, *Adv. Synth. Catal.* **2010**, *352*, 3438–3442.
[15] R. Lingayya, M. Vellakkaran, K. Nagaiah, P. R. Tadikamalla, J. B. Nanubolu, *Chem. Commun.* **2017**, *53*, 1672–1675.
[16] P. Singh, A. G. Cairns, D. E. Adolfsson, J. Ådén, U. H. Sauer, F. Almqvist, *Org. Lett.* **2019**, *21*, 6946–6950.
[17] a) L. A. Paquette, *J. Org. Chem.* **1965**, *30*, 2107–2108; b) R. M. Acheson, P. A. Parker, *J. Chem. Soc. C* **1967**, 1542–1543; c) B. Weinstein, D. N. Brattesani, *J. Org. Chem.* **1967**, *32*, 4107–4108; d) L. Mola, J. Font, L. Bosch, J. Caner, A. M. Costa, G. Etxebarría-Jardí, O. Pineda, D. de Vicente, J. Vilarrasa, *J. Org. Chem.* **2013**, *78*, 5832–5842.
[18] See references therein: L. Rubio-Pérez, R. Azpíroz, A. Di Giuseppe, V. Polo, R. Castarlenas, J. J. Pérez-Torrente, L. A. Oro, *Chem. Eur. J.* **2013**, *19*, 15304–15314.
[19] For C–P see: a) A. Di Giuseppe, R. De Luca, R. Castarlenas, J. J. Pérez-Torrente, M. Crucianelli, L. A. Oro, *Chem. Commun.* **2016**, *52*, 5554–5557; for C–S see: b) L. Palacios, Y. Meheut, M. Galiana-Cameo, M. J. Artigas, A. Di Giuseppe, F. J. Lahoz, V. Polo, R. Castarlenas, J. J. Pérez-Torrente, L. A. Oro, *Organometallics* **2017**, *36*, 2198–2207; for C–N see: c) R. Azpíroz, A. Di Giuseppe, V. Passarelli, J. J. Pérez-Torrente, L. A. Oro, R. Castarlenas, *Organometallics* **2019**, *38*, 1695–1707; for C–O see: d) M. Galiana-Cameo, V. Passarelli, J. J. Pérez-Torrente, A. Di Giuseppe, R. Castarlenas, *Eur. J. Inorg. Chem.* **2021**, 2947–2957.
[20] M. Galiana-Cameo, A. Urriolabeitia, E. Barrenas, V. Passarelli, J. J. Pérez-Torrente, A. Di Giuseppe, V. Polo, R. Castarlenas, *ACS Catal.* **2021**, *11*, 7553–7557.
[21] a) R. Shen, T. Chen, Y. Zhao, R. Qiu, Y. Zhou, S. Yin, X. Wang, M. Goto, L.-B. Han, *J. Am. Chem. Soc.* **2011**, *133*, 17037–17044; b) U. Gellrich, A. Meiβner, A. Steffani, M. Kähny, H.-J. Drexler, D. Heller, D. A. Plattner, B. Breit, *J. Am. Chem. Soc.* **2014**, *136*, 1097–1104; c) L.-J. Song, T. Wang, X. Zhang, L. W. Chung, Y.-D. Wu, *ACS Catal.* **2017**, *7*, 1361–1368.
[22] For an example of hampered C–O reductive elimination within Rh-alkenyl species see: T. D. Marder, D. M.-T. Chan, W. C. Fultz, D. Milstein, *J. Chem. Soc. Chem. Commun.* **1988**, 996–998.
[23] a) H. Chen, D. Harman, *J. Am. Chem. Soc.* **1996**, *118*, 5672–5683; b) M. Zhang, G. Huang, *Chem. Eur. J.* **2016**, *22*, 9356–9365.
[24] L. Palacios, A. Di Giuseppe, R. Castarlenas, F. J. Lahoz, J. J. Pérez-Torrente, L. A. Oro, *Dalton Trans.* **2015**, *44*, 5777–5789.
[25] F. Kakiuchi, S. Takano, T. Kochi, *ACS Catal.* **2018**, *8*, 6127–6137.
[26] Deposition number 2114691 for **2** contains the supplementary crystallographic data for this paper. These data are provided free of charge by the joint Cambridge Crystallographic Data Centre and Fachinformationszentrum Karlsruhe Access Structures service.

Manuscript received: December 13, 2021
Accepted manuscript online: March 8, 2022
Version of record online: March 19, 2022